
Electronic Supplementary Information (ESI)

Amyloid fibril-UiO-66-NH_2 aerogels for environmental remediation

Mohammad Peydayesh[1], Xiulin Chen[1], Julia Vogt[1], Felix Donat[2], Christoph R. Müller[2], and Raffaele Mezzenga*[1,3]

1 Department of Health Sciences and Technology, ETH Zurich, Schmelzbergstrasse 9, 8092 Zurich, Switzerland.

2 Department of Mechanical and Process Engineering, ETH Zurich, Sonneggstrasse 3, 8092 Zurich, Switzerland.

3 Department of Materials, ETH Zurich, Wolfgang-Pauli-Strasse 10, 8093 Zurich, Switzerland.

*Corresponding author: email: raffaele.mezzenga@hest.ethz.ch

Telephone: +41 44 632 9140.

SI Contents

1. Materials and Methods

1.1 Materials

β-Lg was purified from whey protein isolate (Fonterra, New Zealand) and used for amyloid fibril preparation. Zirconium(IV) chloride (≥ 99.9%), 2-aminoterephthalic acid (99%), 1-(2-hydroxyethyl)-2-pyrrolidone (98%), acetic acid (≥ 99.7%), methanol (≥ 99.9%), hydrochloric acid (HCl, 37%), 1,2,3,4-buthanetetracarboxylic acid (BTCA) (99%), sodiumhypophosphate (SHP) (≥ 99%) were all purchased from Sigma Aldrich. To obtain the heavy metal standard solutions, the appropriate amount of gold(III) chloride trihydrate, iron(III) chloride, chloroplatinic acid hydrate, silver nitrate, chromium trioxide, lead(II) nitrate, copper(II) nitrate trihydrate, zinc nitrate hexahydrate, nickel(II) nitrate hexahydrate, and manganese(II) chloride tetrahydrate, which were all supplied by Sigma-Aldrich, were dissolved in Milli-Q water (Milli-Q® purification system, Millipore). Rhodamine B, Crystal violet, Methylene blue, Malachite green for dye aqueous solutions were also purchased from Sigma Aldrich. All other reagents employed in this study were of analytical grade and were purchased from Sigma Aldrich.

1.2 Methods

1.2.1 Preparation of β-Lg amyloid fibrils

Amyloid fibrils of β-Lg were prepared according to the protocol of the previous studies[1]. β-Lg monomers were dispersed homogeneously in Milli-Q water with a concentration of 2 wt.%, following the adjustment of pH with HCl (1 M) to pH 2. Afterward, the β-Lg solution was incubated at 90°C for 5 h with constant magnetic stirring at 350 rpm. Then, the solution was immediately immersed in ice-water mixtures to stop the fibrillation process. Ultimately, the presence of β-Lg amyloid fibrils was verified by the birefringence via the cross-polarized light.

1.2.2 Preparation of UiO-66-NH_2

2-aminoterephthalic acid (498 mg) was dissolved in 24 mL 1-(2-hydroxyethyl)-2-pyrrolidone, which is a green solvent compared with DMF[2]. Then 162 μL water, 5160 μL acetic acid, and 696 mg $ZrCl_4$ were added into the solution. The mixture was sonicated and the suspension was then transferred to a 50 mL autoclave and placed in a thermostated oven at 120 °C for 24 h. After completion of the reaction, the solid was centrifuged at 10000 rpm for 10 min and washed with methanol and water.

1.2.3 Preparation of the hybrid aerogel

To manufacture the cross-linked hybrid aerogels, BTCA was first added into amyloid fibrils as the crosslinker (an amyloid fibril to BTCA weight ratio of 1:0.2). Then, SHP was added as the catalyst (an SHP to BTCA weight ratio of 2:1). After the dispersion was completed, UiO-66-NH_2 was added into the solution, with an amyloid fibril to UiO-66-NH_2 weight ratio of 4:1. The solution was slowly stirred to avoid breaking the fibrils until UiO-66-NH_2 was completely dispersed. For fabricating aerogels, the mixture was purred into 2 ml stainless-steel molds. The samples were frozen at -18°C and subsequently were freeze-dried (FreeZone Plus 4.5, Labconco, United States). Finally, the freeze-dried aerogels were heated at 150°C for 5 min to achieve cross-linking[3].

1.2.4 Characterization of UiO-66-NH_2 and hybrid aerogel

Transmission electron microscopy (TEM, Talos F200X, FEU) images and the elemental map of the UiO-66-NH_2 were obtained at accelerating voltages of 80 kV. A diluted solution of UiO-66-NH_2 (4 μL) was dripped on Ultrathin Carbon Film Coated Lacey Carbon Supported Copper Grid (Sigma Aldrich) before TEM measurements. The Zeta potential of UiO-66-NH_2 was measured at different pH values (2 to 12) by Malvern Nano-Zetasizer® to determine the charge of UiO-66-NH_2. The surface area and total pore volume of UiO-66-NH_2 were determined by N_2 adsorption-desorption at

-196 °C according to Brunauer-Emmett-Teller (BET) method (Micromeritics II Plus, USA). The samples were degassed under N_2 at 150 °C for 24 h before measurements.

The inner structure and morphology of the hybrid aerogel were determined by a Hitachi SU5000 Scanning Electron Microscopy (SEM). The aerogel was broken into small pieces within liquid nitrogen without stretching the structure. The aerogel was sputter-coated with 5 nm of platinum/palladium before imaging (Safematic, CCU-10, Switzerland). X-ray diffraction (XRD) patterns of amyloid fibrils, hybrid aerogel, and UiO-66-NH_2 were recorded with a PANalytical Empyrean X-ray diffractometer to investigate the crystalline phases. The instrument was equipped with an X'Celerator Scientific ultra-fast line detector and Bragg-Brentano HD incident beam optics using Cu Kα radiation (45 kV and 40 mA). Measurements were conducted in the 2θ range 4 - 70° with a step size of 0.0167°. Each measurement lasted 30 min. Fourier transform infrared (FTIR) spectra of amyloid aerogel, hybrid aerogel, and UiO-66-NH_2 were obtained using a Nicolet iS50 FTIR spectrometer (Thermo Scientific) equipped with an ATR module. The spectra were measured in the range from 650 to 4000 cm^{-1}. The mechanical properties of the hybrid aerogel were measured using a Z010 (Zwick) with two flat surface compression stages and a 10 N load cell. The compressive strain-stress curves measurements were conducted at a maximum strain of 60%.

1.2.5 Water purification

Heavy Metals Adsorption. The working heavy metal solutions were freshly prepared by diluting standard solutions with Milli-Q water to achieve the required concentrations. The removal efficiency R (%) was measured by immersing one aerogel (around 50 mg) into 10 mL of each heavy metal solution (50 ppm) individually. The initial and final concentrations of the heavy metal ions were determined in solution using an atomic absorption spectroscopy (AAS) machine (Agilent AA240Z Zeeman graphite-furnace (GTA 120) equipped with PSD 120 programmable sample dispenser). The removal efficiency R (%) was calculated using equation (1):

$$R(\%) = \frac{C_0 - C_e}{C_0} \times 100$$

(1)

where C_0 and C_e (mg/L) are the initial and final concentrations of the heavy metal ions, respectively.

The maximum adsorption capacity q (mg/g) was measured by immersing one aerogel into 10 mL of each heavy metal solution (10000 ppm) individually. q was calculated by equation (2):

$$q = \frac{C_0 - C_e}{m} V$$

(2)

where V (L) is the volume of the heavy metal solution, and m (g) is the weight of the hybrid aerogel.

For binding isotherm, the same amounts of aerogels (50 mg) were immersed into Au solutions with concentrations of 50, 500, 2000, 5000, 10000 ppm, respectively. For all aforementioned experiments, the aerogels were kept in heavy metal solutions for 24 h. The binding isotherm was fitted according to equation (3)[4]:

$$[P \cdot L] = \frac{1}{2}\left([P_0] + [L_0] + \frac{1}{K_a}\right) - \frac{1}{2}\sqrt{\left([P_0] + [L_0] + \frac{1}{K_a}\right)^2 - 4[MP_0][L_0]} \quad (3)$$

A single binding metal-ligand pair with a single average binding constant was simulated in this method. *[P]* and *[L]* are the bound Au^{3+} and ligand concentrations, respectively. $[P_0]$ and $[L_0]$ are the initial Au^{3+} and ligand concentration, and K_a is the binding constant.

Dyes Adsorption. The maximum dye removal capacity was determined by immersing one aerogel into 5 mL of each dye (1000 ppm) for 24 h. UV-vis spectrometer (Cary Series, Agilent Technologies) was used to measure the initial and final concentration of dye. The maximum dye removal capacity was calculated by equation (2) as that for

heavy metals.

Organics Adsorption. Four drops of *n*-hexane (stained with Oil Red O) were dripped onto the water surface and a small piece of aerogel was contacted with *n*-hexane until finishing adsorption.

Regeneration. Crystal violet, Fe^{3+}, and Pt^{4+} were used as model compounds. Aerogels were immersed in 50 ppm Crystal violet, Fe^{3+}, and Pt^{4+} solution for 24 h, respectively, and then washed for 24 h with HCl (1 M) for Fe^{3+} and Pt^{4+}, and methanol anhydrous for Crystal violet. The HCl and methanol anhydrous were replaced periodically during washing. The aerogels were rinsed with Milli-Q water for 30 min after washing. The initial and final concentrations were measured for three consecutive cycles. The removal performances were calculated by equation (1).

1.2.6 CO_2 capture

A thermogravimetric analyzer (TGA) equipped with a DSC sensor (Mettler Toledo TGA/DSC 3+) was used to investigate the CO_2 sorption properties of amyloid aerogel, hybrid aerogel, and UiO-66-NH_2. Samples were placed in a 150 μL Pt crucible and heated to 150 °C in pure N_2 for 60 min. Three consecutive cycles of CO_2 sorption (at 30°C, pCO_2 = 1 bar, 40 min) and CO_2 release (at 150°C, pure N_2, 60 min) were performed. The total flow rate of gas into the TGA was 150 mL/min, controlled using mass flow controllers (Bronkhorst, EL-Flow) at ambient temperature and pressure. Blank measurements using the empty Pt crucible only were performed under identical conditions for correction.

2. Supporting Figures

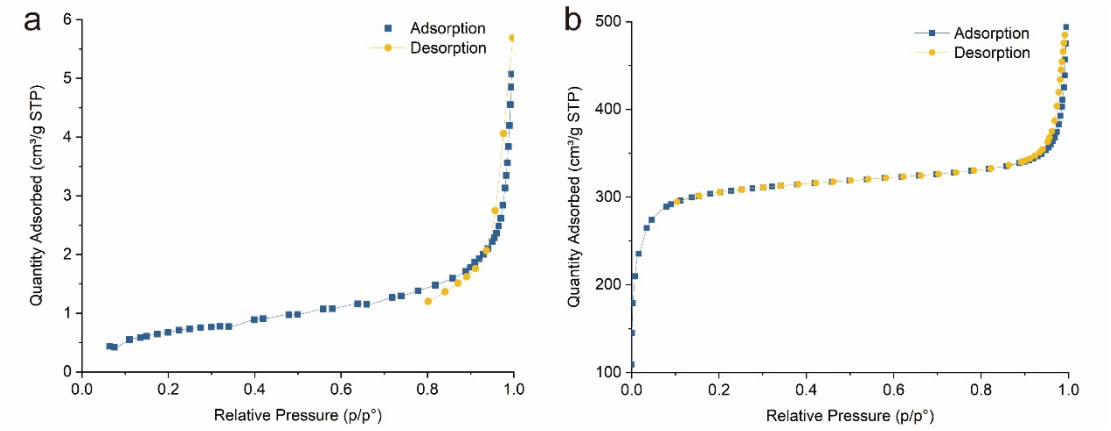

Figure S1. a) N_2 sorption isotherm of the hybrid aerogel and b) UiO-66-NH_2.

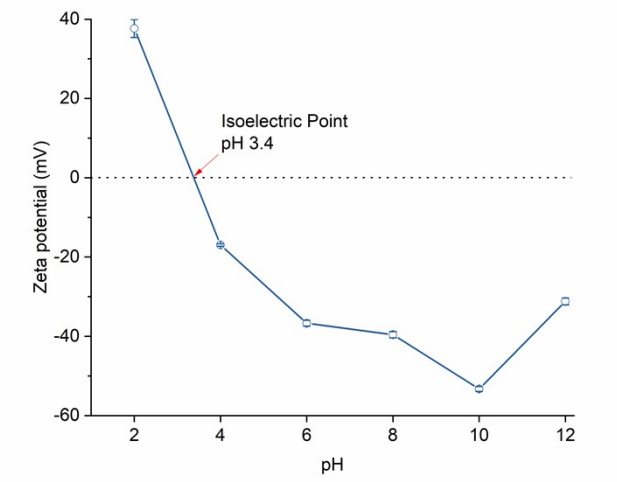

Figure S2. Zeta potential of UiO-66-NH_2 at different pH values.

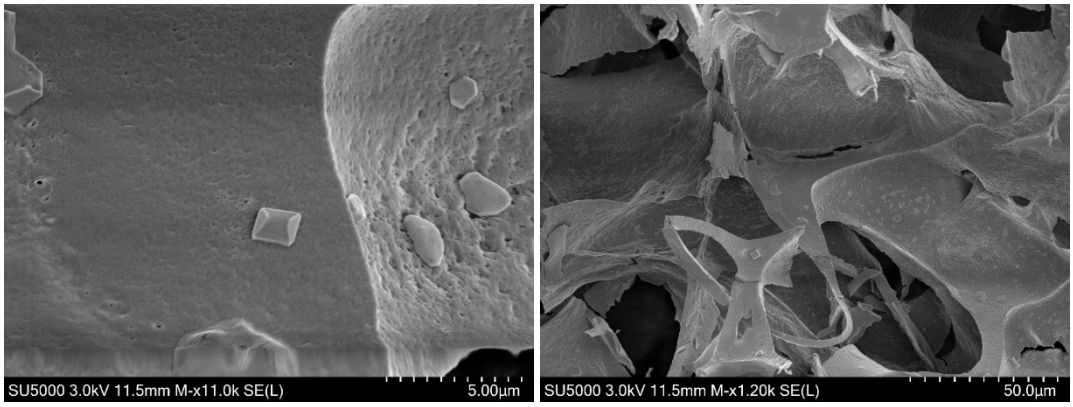

Figure S3. SEM images of the internal structure of hybrid aerogel.

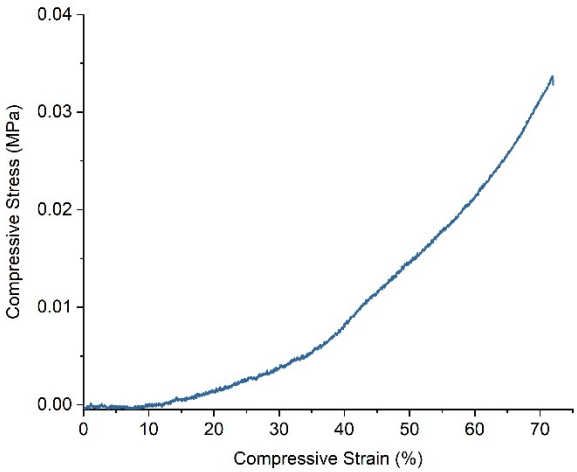

Figure S4. Compressive strain and stress curve of the hybrid aerogel.

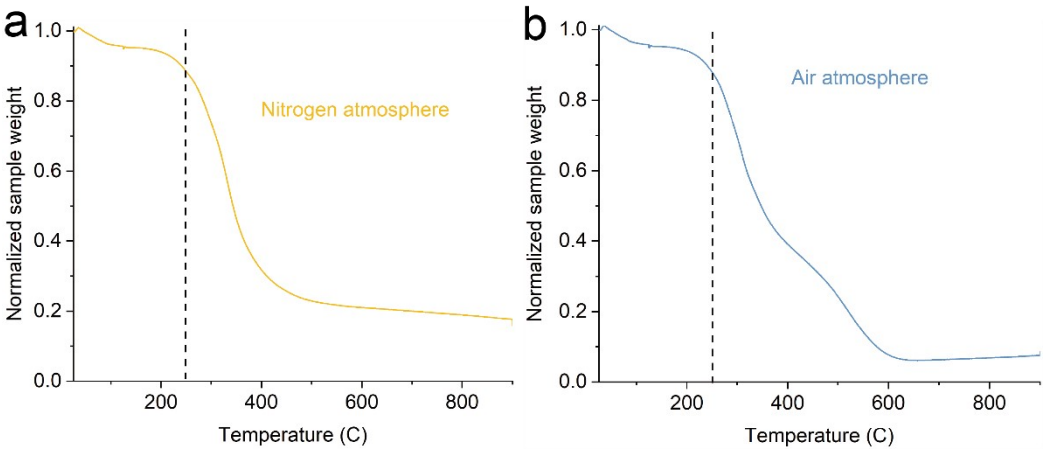

Figure S5. TGA curves of the hybrid aerogel in a) nitrogen and b) air atmosphere. The residue obtained after the complete decomposition is given by remaining salts in the system, added during crosslinking and adjustment of pH.

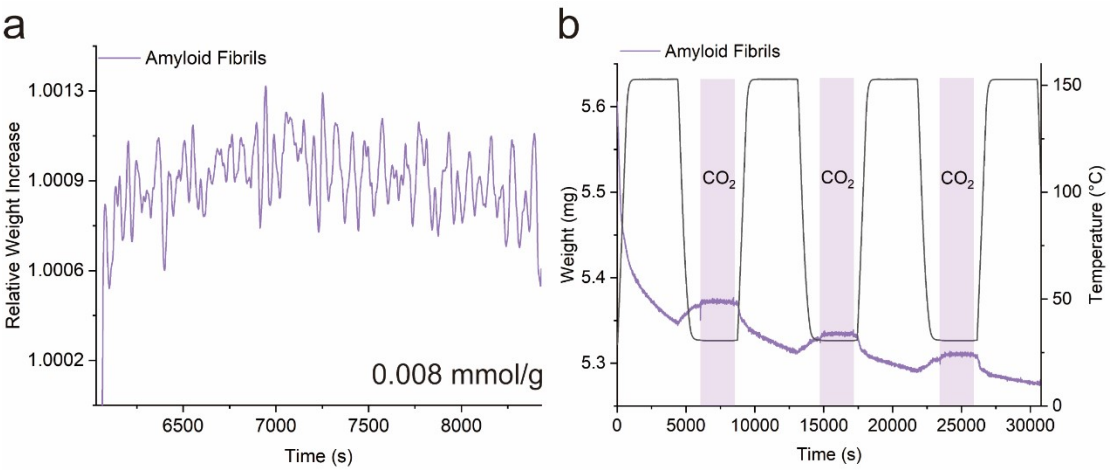

Figure S6. CO_2 capture performance of pure amyloid fibrils. a) relative weight increase after the first cycle of CO_2 sorption. b) weight changes for three consecutive cycles of CO_2 sorption-desorption. The CO_2 sorption part is highlighted by colored backgrounds.

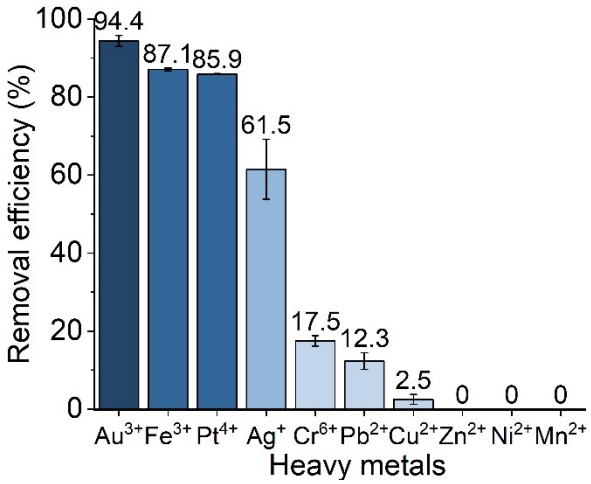

Figure S7. Heavy metal removal efficiency of the hybrid aerogel.

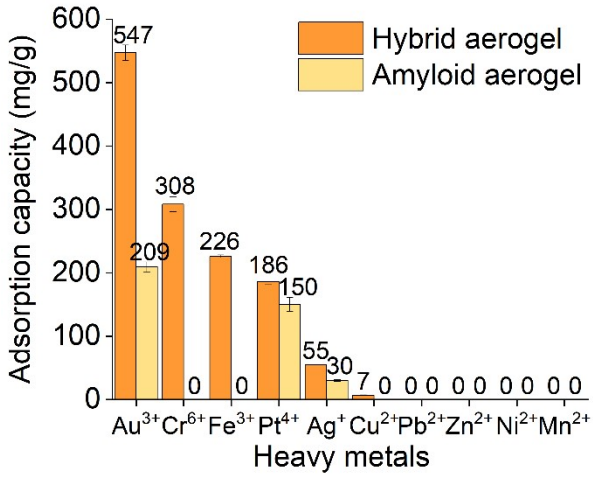

Figure S8. Heavy metal adsorption capacity of the hybrid aerogel and amyloid aerogel.

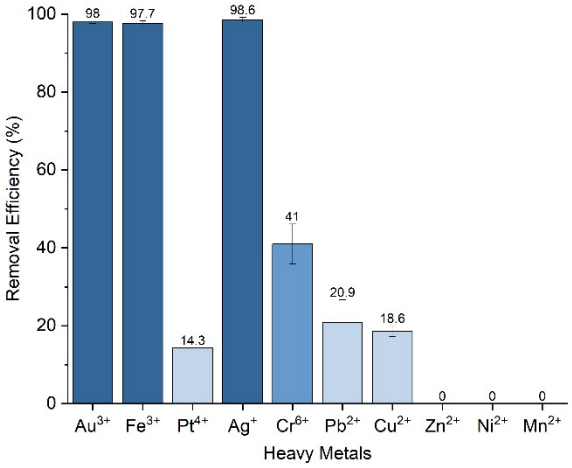

Figure S9. The removal efficiency of the hybrid aerogels for heavy metals mixture, 5 ppm for each heavy metal and 50 ppm in total.

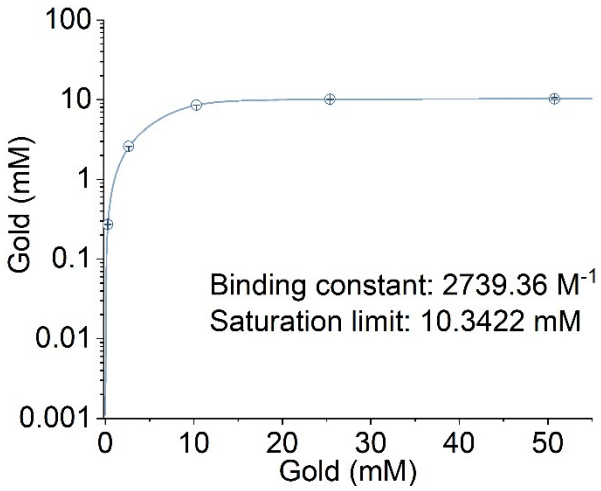

Figure S10. Fitted binding isotherm of Au^{3+} (equilibrium concentrations vs. initial concentrations).

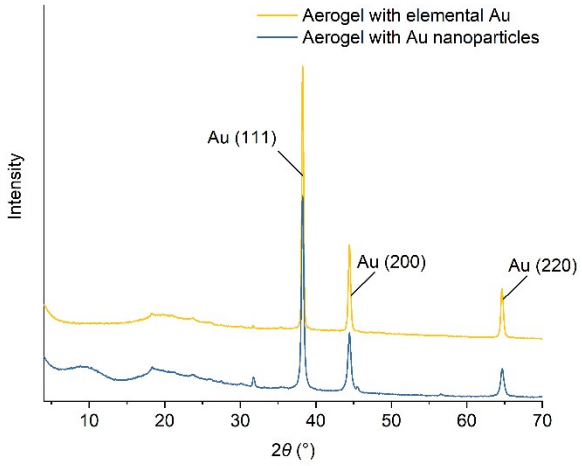

Figure S11. XRD patterns of hybrid aerogels after adsorbing different concentrations of Au^{3+}.

3. Supporting Tables

Table S1. BET results of the UiO-66-NH_2 and the hybrid aerogel.

BET	UiO-66-NH_2	Hybrid Aerogel
Surface area (m^2/g)	966.7 ± 9.3	2.1 ± 0.3
Pore radius (Å)	7.1 ± 0.01	6.3 ± 0.1
Pore Volume (cm^3/g)	0.3 ± 2.6 × 10^{-3}	6.4 × 10^{-4} ± 4 × 10^{-5}

Table S2. Mechanical strength of the hybrid aerogel.

Mechanical Strength	Hybrid Aerogel
Density (mg/cm^3)	40.6 ± 2.4
Max Stress (MPa)	$3.4 \times 10^{-2} \pm 1 \times 10^{-4}$
Max Strain (%)	$59.5 \pm 1.7 \times 10^{-3}$
E (Mpa)	$2 \times 10^{-2} \pm 1.8 \times 10^{-3}$
Specific Strength (kNm/kg)	$0.8 \pm 5.3 \times 10^{-2}$
Specific Stiffness (MNm/kg)	$4.9 \times 10^{-4} \pm 1.5 \times 10^{-5}$

Table S3. Au^{3+} adsorption capacity of various kinds of adsorbents.

Adsorbents	Adsorption capacity (mg/g)
UiO-66-NH_2	166[5]
UiO-66-MTD	302[6]
UiO-66-TA	372[7]
Graphene/carbon nanotube aerogels	47[8]
Amyloid fibrils	209 (This work)
UiO-66-NH_2/amyloid aerogels	547 (This work)

References

1. Jung, J.-M.; Savin, G.; Pouzot, M.; Schmitt, C.; Mezzenga, R.,. *Biomacromolecules* 2008, ***9*** (9), 2477-2486.

2. Morelli Venturi, D.; Campana, F.; Marmottini, F.; Costantino, F.; Vaccaro, L., *ACS Sustain. Chem. Eng.* 2020, ***8*** (46), 17154-17164.

3. Nyström, G.; Fong, W.-K.; Mezzenga, R., *Biomacromolecules* 2017, ***18*** (9), 2858-2865.

4. Motulsky, H., The GraphPad guide to nonlinear regression. *GraphPad Prism Software User Manual, GraphPad Software Inc., San Diego, CA* 1996.

5. Zhao, M.; Huang, Z.; Wang, S.; Zhang, L.; Wang, C.,. *Micropor. Mesopor. Mat.* 2020, ***294***, 109905.

6. Wang, C.; Lin, G.; Zhao, J.; Wang, S.; Zhang, L.,. *Chem. Eng. J.* 2020, ***388***, 124221.

7. Wang, C.; Lin, G.; Zhao, J.; Wang, S.; Zhang, L.; Xi, Y.; Li, X.; Ying, Y., *Chem. Eng. J.* 2020, ***380*****,** 122511.

8. Wang, S.; Shen, M.; Qu, J.; Zhuang, X.; Ni, S.-Q.; Wu, X., *J. Non-Cryst. Solids* 2020, ***536***, 120008.